Biomimetic Cytomembrane Nanovaccine Prevents Breast Cancer Development in the Long Term

Long Xiao‡[a], Yu Huang‡[b], Yuhe Yang‡[c], Zhiwei Miao‡[a], Jie Zhu[a], Mengdan Zhong[a], Chencheng Feng[a], Wenkai Tang[a], Jinhua Zhou*[b], Lihong Wang*[a], Xin Zhao*[c], Zhirong Wang*[a]

Cytomembrane cancer nanovaccines are considered a promising approach to induce tumor-specific immunity. Most of currently developed nanovaccines, unfortunately, fail to study the underlying mechanism for cancer prevention and therapy, as well as immune memory establishment, with their long-term anti-tumor immunity remaining unknown. Here, we present a strategy to prepare biomimetic cytomembrane nanovaccines (named as CCMP@R837) consisting of antigenic cancer cell membrane (CCM) capped poly (lactic-co-glycolic acid) (PLGA) nanoparticles loaded with imiquimod (R@837) as adjuvant to activate immune system. We found that our CCMP@R837 system enhanced bone-marrow derived dendritic cell uptake and maturation, as well as increased anti-tumor response against breast cancer 4T1 cells in vitro. Moreover, an immune memory was established after a three-time immunization with CCMP@R837 in BALB/c mice. The CCMP@R837 immunized BALB/c mice exhibited suppressed tumor growth and long survival period (75% of mice lives longer than 50 days after tumor formation). This long-term anti-tumor immunity was achieved by increasing $CD8^+$ T cells and decreasing regulatory T cells in the tumor, while raising effector memory T cells in the spleen. Overall, our platform demonstrates that the CCMP@R837 can be a potential candidate for the preventive cancer vaccine in clinic.

Introduction

Training the autologous immune system using cancer cell membrane (CCM) vaccines to recognize and fight cancers, is a promising modality for cancer prevention and therapy [1-7]. This strategy takes advantage of the natural capability of cytotoxic T lymphocytes (CTLs) to recognize the diverse receptors on the CCM, increasing their specificity to fight against tumor cells and reducing side effects [6, 8-12]. Moreover, it has a relatively low cost as fashioning CCM directly into nanoparticle (NP) format bypasses the heavy workload of proteomics [13] and the engineering hurdles behind functionalizing NPs [8]. Recently, several studies have encapsulated NPs (e.g., metal-organic framework (MOF) NPs [14], gold NPs [15], poly (lactic-co-glycolic acid) (PLGA) NPs [16], with various CCM (e.g., 4T1 cells, dendritic cells (DCs), B16-F10 cells) for the purposes of cancer prevention and therapy. Most of the above-mentioned studies, however, did not examine the DC activation and the immune memory establishment using the nanovaccine strategies and the underlying mechanism of these approaches for cancer prevention and therapy, as well as their long-term anti-tumor immunity, remain unknown [6, 14-17].

In this study, we encapsulate biodegradable PLGA NPs loading R837 (an agonist against toll-like receptor 7) [18] as adjuvant with 4T1 CCM as antigens. We demonstrate that the resulting NPs (denoted as CCMP@R837) possess an antigenic shell closely resembling the source cancer cells. Compared to its naked counterparts, our CCMP@R837 shows enhanced bone marrow derived dendritic cell (BMDC) uptake and stronger stimulation effect to trigger secretion of interleukin-12 (IL-12p70), which further stimulates the Tissue-resident memory T (Trm) cells to secrete effector molecules interferon (IFN)-γ and tumor necrosis factor (TNF)-α to achieve the anti-tumor effects (Scheme 1). The mature DCs are found to suppress Treg differentiation from naïve $CD4^+$ T cells while activating the naïve $CD8^+$ T cells, making them massively proliferate and differentiate into central-memory (T_{CM}) and effector-memory (T_{EM}) $CD8^+$ T cells. When the immunized mice (treated using CCMP@R837) is challenged with 4T1 cancer cells, the pre-trained immune system recognizes and destroys cancer cells, with long-lasting anti-tumor immunity. Our work highlights the great potential of the CCMP@R837 to develop nanovaccines for cancer immunotherapy.

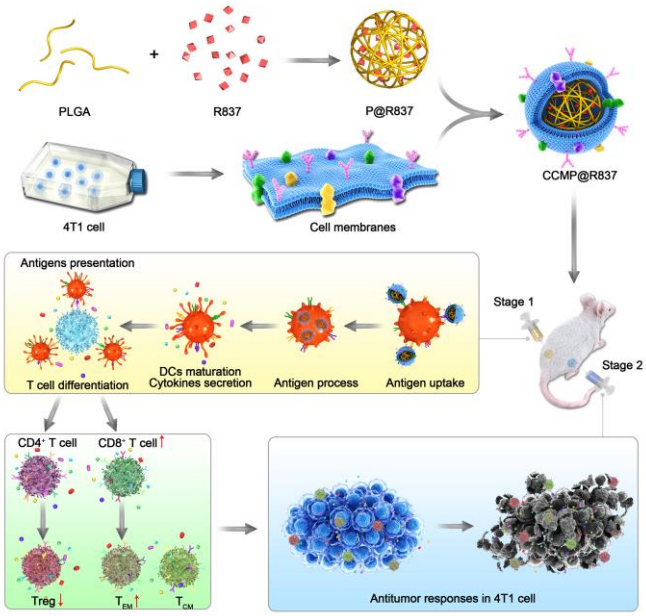

Scheme 1. Fabrication and mechanism of cancer immunotherapy of CCMP@R837. CCMP@R837 are fabricated by encapsulating biodegradable poly (lactic-co-glycolic acid) (PLGA) nanoparticles (NPs) loading R837 (an agonist against toll-like receptor 7) as adjuvant with 4T1 cancer cell membrane as antigens. When the nanovaccines are injected into a mouse model (stage 1), they will be uptaken by dendritic cells (DCs) and trigger the DCs to secrete cytokines (e.g., interleukin-12), which will then suppress Treg differentiation from naïve $CD4^+$ T cells and activate the naïve $CD8^+$ T cells to differentiate into central-memory (T_{CM}) and effector-memory (T_{EM}) $CD8^+$ T cells. When the immunized mouse is challenged with 4T1 cancer cells (stage 2), the T_{CM} and T_{EM} cells will differentiate into cytotoxic T lymphocytes (CTLs) to recognize and destroy cancer cells, with long-lasting anti-tumor immunity.

Materials and methods

Materials

PLGA, dimethyl sulfoxide (DMSO) and dichloromethane (CH2Cl2) were purchased from Sigma-aldrich; R837 (Imquimod) was obtained from InvivoGen; All the antibodies for flow cytometry and Zombie aqua fixable viability kit were obtained from Biolegend; IL-12p70, IFN-γ and TNF-α ELISA kits were purchased from Thermo Fisher.

Cell line

4T1 mouse breast cancer cell line was acquired from the American Type Culture Collection (ATCC). 4T1 cells were cultured in the Roswell Park Memorial Institute (RPMI) 1640 medium (HyClone) supplemented with 10 % fetal bovine serum (FBS, Gibco), penicillin (100 U/mL HyClone), and streptomycin (100 U/mL; HyClone). BMDCs were isolated from the tibia and femur of the BLAB/c mice (4-6 weeks) according to an established method [19] and cultured with the same condition as 4T1.

Animal

Female BALB/c mice (4-6 weeks) were purchased from Shanghai Biomodel Organism Science & Technology Development Co., Ltd. and treated under protocols approved by the Institute of Animal Care Committee of Zhangjiagang Traditional Chinese Medicine Hospital (approval number: 2019A011), in accordance with international ethics guidelines and the National Institutes of Health of China, concerning the Care and Use of Laboratory Animals.

Cell membrane isolation

4T1 cells were cultured in T75 flasks (Thermo Fisher) until the cells were 80 % confluent. The cells were detached with PBS-EDTA (Gibco, Thermo Fisher) followed by washing with 1× PBS (HyClone) three times. Afterwards, the obtained pellet was resuspended in a hypotonic lysing buffer with 1 tablet protease inhibitor (Thermo Fisher). Finally, gradient centrifugation (20,000 g for 30 min and 100,000 g for 20 min) was used to get the 4T1 cell membrane pellet for the further use [20].

Synthesis of CCMP@R837

P@R837 NPs were fabricated as previously reported [5]. Briefly, PLGA (25 mg/mL) was dissolved in CH2Cl2 with 200 μg R837 (in DMSO at 5 mg/mL), then 0.5 mL polyvinylpyrrolidone (PVP) solution (5 % w/v) was added into the PLGA mixture followed by tip-sonication (40 % power for 3 minutes, 3 seconds on and 1 second off). After that, 2.5 mL PVP solution (5% w/v) was added dropwise into the obtained solution under constant stirring overnight at room temperature. The P@R837 NPs were obtained after centrifugation at 3,500 g for 25 min. The naked PLGA NPs (denoted as P) were fabricated using the same protocol, without adding the R837. To prepare CCMP@R837, 4T1 cell membrane pellet was bath-sonicated and physically co-extruded with P@R837 through a 200 nm polycarbonate membrane (Avanti Lipids) by mini extruder (Avanti Lipids) for 11 passes. Fluorescence labelled P, P@R837 and CCMP@R837 were named as F#P, F#P@R837 and F#CCMP@R837. These NPs were prepared by adding coumarin 6 into the solution of PLGA.

Characterization of physical properties of CCMP@R837

The hydrodynamic size and zeta potentials of CCM, P@R837, and CCMP@R837 were explored using a Zetasizer Nano-ZS (Malvern Instruments) with dynamic light scattering (DLS) and electrophoretic light scattering (ELS), respectively. The protein content of CCMP@R837 was investigated by the micro (bicinchoninic acid) BCA assay kit. Additionally, the long-term stability of CCMP@R837 (stored at 4℃ without stirring in 1×PBS) was investigated using DLS. The release behaviour of CCMP@R837 was explored by high-performance liquid chromatography (HPLC) with an ultraviolet-visible detector at 325 nm. The morphology of CCMP@R837 was visualized using transmission electron microscope (TEM, FEI).

Characterization of in vitro biological properties of CCMP@R837

The biocompatibility of CCMP@R837 was investigated in both BMDCs and 4T1 cells. Briefly, BMDCs (1×10^4 cells/well in 96 well plate) and 4T1 cell (1×10^4 cells/well in 96 well plate) were respectively treated with different formulas (CCM, P@R837, and CCMP@R837, P@R837 and CCMP@R837 contained the same amount of R837/well) for 1, 2 and 3 days. NC means cells cultured without any NPs. Cell viability was assessed using CellTiter-Glo reagent assay (Promega Corporation) according to the manufacturer's instructions.

To quantify the BMDCs' uptake, F# P, F#P@R837 and F#CCMP@R837 were co-cultured with BMDCs (3×10^5 cells/well in 24 well plate) for 1, 6 and 24 hours. After incubation, the BMDCs were detached and washed with 1×PBS, then trypan blue was used to eliminate any NPs bound onto the surface of BMDCs before flow cytometry analysis (BD, FACS Celesta).

The ability of CCMP@R837 in inducing BMDC activation was further explored by treating BMDCs with different formulations (R837, CCM, P@R837 and CCMP@R837, respectively) for 1, 2 and 3 days in vitro. After incubation, the BMDCs were detached and washed with 1×PBS, then stained with CD11c-FITC, CD80-PE, and CD86-APC for further flow cytometry analysis. To further explore the immune activation ability of CCMP@R837, BMDCs were firstly treated with different formulations (R837, CCM, P@R837, R837+CCM, and CCMP@R837). After 3 days' treatment, BMDCs were detached and washed with 1×PBS. Then these BMDCs were co-cultured with splenocytes for another 3 days; this treatment made BMDCs process and presented the related antigens to splenocytes. Finally, both BMDCs and splenocytes were collected and co-cultured with 4T1 cells for 24 hours. After that, the culture medium suspension was collected to evaluate the concentration of IFN-γ and IL-12p70 by ELISA kit, and the 4T1 cells were gently washed three times using the 1×PBS, and the cell viability of 4T1 was evaluated by the CellTiter-Glo reagent assay.

Immunogenicity of CCMP@R837

Female BALB/c mice (randomly divided into four groups) were subcutaneously treated with different formulations (Saline, CCM, P@R837 and CCMP@R837) on day 0, 14, and 28. The body weight of mice was recorded every two days. Three days after the pre-immunization, 4T1 cells were subcutaneously injected into the right flank of these mice. Then the tumor size and the survival rate of each mice were recorded every two days. 14 days post the 4T1 cell injection, five mice were randomly selected from each group to analyze the immunological profile of the tumor tissue, inguinal lymph nodes and the concentration of TNF-α in the blood. Specifically, the peripheral blood was collected from each mice and serum was isolated to analyze the concentration of TNF-α by ELISA. Afterwards, mice were euthanized, and the tumor tissue and inguinal lymph nodes were collected respectively to prepare the single cell suspension for flow cytometry analysis as described elsewhere [5]. Firstly, the zombie aqua fixable viability kit was used to gate the living cells, then the differentiated hematopoietic cells were gated in $CD45^+$ population (as a marker for the leukocytes). On the one hand, cytotoxic T lymphocytes (CTLs) were gated in $CD45^+$, $CD3^+$, and $CD8^+$ (CD3 as a marker for both cytotoxic T cell and T helper cells, CD8 as a marker for cytotoxic T cells) [21]. The subpopulation of CTLs was further analyzed in central memory T cells (T_{CM}, $CD62L^+CD44^+$) and effector memory T cells (T_{EM}, $CD62L^-CD44^+$) to explore the main subpopulation in inhibiting cancer cells. On the other hand, helper T cells was gated in $CD45^+$, $CD3^+$, and $CD4^+$, while the regulatory T cells (Treg) was gated in $CD3^+$, $CD4^+$, and $Foxp3^+$ (CD4 as a marker for T helper cells, $Foxp3^+$ as a marker for the regulatory T cells). Immunohistochemistry was used to evaluate the T cell subpopulation ($CD3^+$, $CD4^+$ and $CD8^+$) and distribution of these subpopulations in the tumor area of mice treated with CCMP@R837. 21 days after the 4T1 injection, three mice were randomly selected from each group, and the tumor size was qualitatively investigated using the small animal in vivo optical imaging [22].

Statistical analysis

To compare differences between groups, one-way ANOVA with Tukey's multiple comparison test was used (IBM SPSS Statistics 25). *p < 0.05, **p < 0.01 and ***p < 0.001 indicate statistically significant. Values are expressed as mean ± SD.

Results and discussion

Physical characteristics of CCMP@R837

In this study, we fabricated PLGA NPs loading R837 as adjuvant with 4T1 CCM as antigens, denoted as CCMP@R837. PLGA NPs loading R837 (denoted as P@R837) and naked PLGA NPs (denoted as P) were used as control. To investigate if the CCM coating was successful, we first characterized the morphology of the prepared NPs. The CCMP@R837 showed a core-shell structure (Fig. 1a), where the dark part was the P@R837 core and the light coating was the CCM. We then examined the diameter and zeta potential of different NPs [23]. The DLS (Fig. 1b) and the ELS (Fig. 1c) results indicated that the average diameter of CCMP@R837 (164.2 ± 5.9 nm) was larger than P@R837 (122.4 ± 4.2 nm), due to the presence of CCM coating. In addition, the zeta potential increased from -40.6±1.1 mV for P@R837 to -20.4±2.6 mV for CCMP@R837 due to the presence of CCM (-19.5±1.1 mV) on the surface of P@R837. Further, we checked the protein content of CCMP@R837 in comparison to the cell membrane by the micro BCA protein assay, and we found that every 1 mg CCMP@R837 included 0.6 mg proteins. In addition, it was found that after 28 days of storage at 4℃, the diameter of CCMP@R837 exhibited negligible change, indicating the long-term stability of these NPs (Fig. 1d). We then investigated the drug release from CCMP@R837 (Fig. 1e). We first investigated the loading efficacy of R837 in CCMP@R837 and it was found to be 7.3±1.1%. We then found that after first 24 hours of immersion in phosphate buffered saline (PBS), over 50% of loaded R837 was released, and after 72 hours, almost all R837 (93.2±3.45%) was released. The above data indicated that the CCMP@R837 was successfully synthesized.

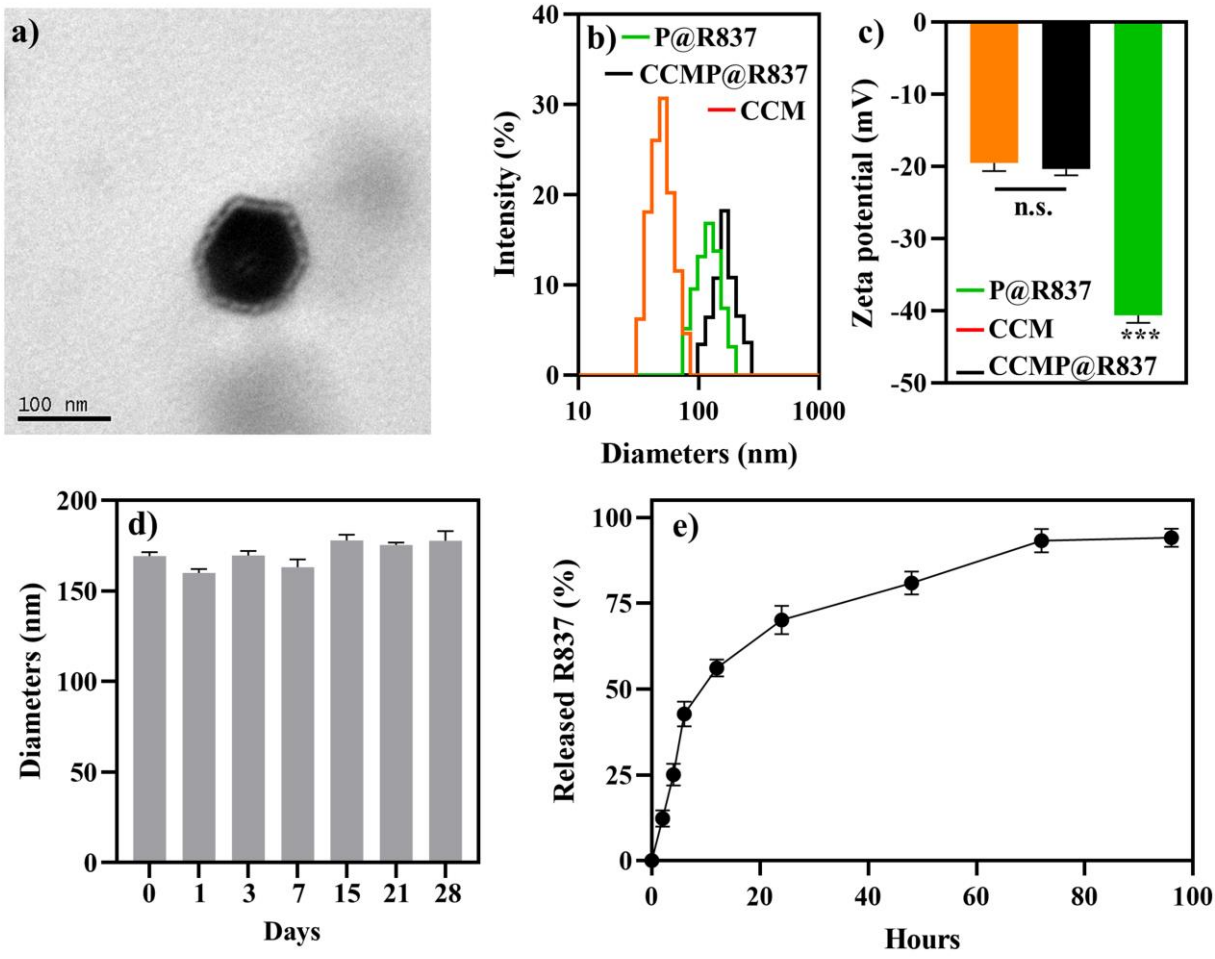

Fig. 1. Physical characteristics of CCMP@R837. a) Morphology of resultant CCMP@R837 NPs. b) Hydrodynamic diameter of CCM, P@R837, and CCMP@R837. c) Surface zeta potential of CCM, P@R837, and CCMP@R837 d) Hydrodynamic diameter of CCMP@R837 at 4℃ in 1×PBS for 28 days. e) R837 release from CCMP@R837 in vitro. Data represent mean ± SD (n =3). Please note that there is no significant difference between P@R837 and CCM, but significant difference between CCMP@R837 and P@R837 / CCM groups was observed (***p < 0.001).

Biocompatibility and Cellular Uptake of CCMP@R837

After successful synthesis of CCMP@R837, we examined the biocompatibility of these NPs using BMDCs and 4T1 cells. BMDC was selected as a model immune cell to evaluate the biocompatibility of the system while 4T1 cells was used to investigate whether the system was cytotoxic to cancer cells. As shown in Fig. S1a, BMDCs treated with various formulations exhibited similar cell viability (around 100 % compared with the negative control groups, NC, culture medium) except for the positive control (PC) groups treated with 1% Triton X-100 (the cell viability in PC groups was around 10 %). Similar trend was observed in the 4T1 cells treated with different formulations (Fig. S-1b). These results suggested that the CCM, P@R837, and CCMP@R837 were not cytotoxic for both BMDCs and 4T1 cells in vitro. We further evaluated the BMDCs' uptake of these NPs using flow cytometry (Fig. S-1c). From 1 to 24 hours, an enhanced cellular uptake was found in the BMDCs treated with CCMP@R837 compared with P@R837, suggesting that the presence of CCM can enhance the BMDC uptake. Additionally, comparing the uptake percentage of P and P@R837, more uptake percentage could be found in the P@R837, which could be attributed to the immunogenic properties of R837.

Immunogenicity of CCMP@R837 in vitro

After the cellular uptake investigations, the efficacy of CCMP@R837 boosting the $CD86^+$ and $CD80^+$ expression in BMDCs (indicating BMDC activation) was evaluated in vitro using flow cytometry. As shown in Fig. 2a, after 1 day of incubation, there was no significant maturation difference between the BMDCs treated with formulations containing R837 or not; whereas, after 2 days of incubation, BMDCs treated with CCMP@R837 exhibited higher maturation percentage (81.7 ± 2.2% in CD86+, 78.9 ± 2.5% in $CD80^+$) than those treated with R@837 (67.8 ± 5.5% in $CD86^+$, 52.7 ± 3.7% in $CD80^+$) and P@R837 (64.2 ± 4.0% in $CD86^+$, 55.4 ± 4.8% in $CD80^+$). Similarly, after three days of incubation, BMDCs treated with CCMP@R837 showed much higher maturation percentage (88.9 ± 2.5% in $CD86^+$, 80.0 ± 4.5% in $CD80^+$) than those treated with R@837 (69.5 ± 4.2% in $CD86^+$, 67.9 ± 6.7% in $CD80^+$) and P@R837 (75.2 ± 4.1% in $CD86^+$, 68.7 ± 3.9% in $CD80^+$). The increased maturation percentage in BMDCs treated with CCMP@R837 indicated that the co-delivery of antigens and adjuvant within the same nanocarriers can significantly boost BMDC activation, which is vital for immunogenicity [16, 24].

To verify whether the CCMP@R837 could trigger enhanced immune response, the BMDCs were treated with different formulations for inducing BMDC activation and antigen processing. As demonstrated in Fig. 2b, specifically, BMDCs were treated with the mixture of CCM and R837 as a control to explore whether the CCMP@R837 would induce stronger immune response than the control. BMDCs cultured only with medium were used as NC. After three days' treatment, BMDCs were co-cultured with splenocytes for another three days to activate the T cells in the splenocytes, then both the BMDCs and the splenocytes were further co-cultured with 4T1 cells to investigate whether the induced T cells can kill 4T1 cancer cells. We then collect the suspension (medium of 4T1 cultured with BMDCs and splenocytes) to explore the mechanism underlying inhibition of cancer cell growth. As shown in Fig. 2c, the viability of 4T1 cells treated with NC groups were regarded

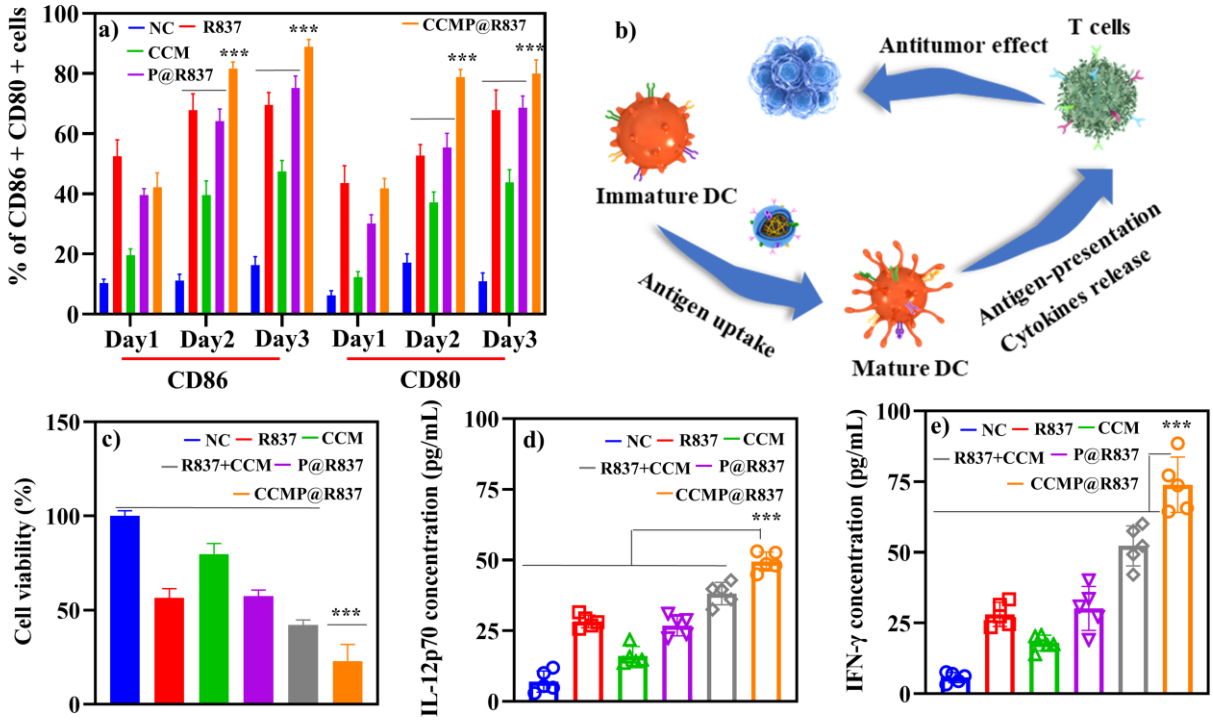

as 100 %. We found that the 4T1 cells treated with CCMP@R837 exhibited the lowest cell viability compared to R837+CCM groups (mixture of R837 and CCM), indicating that the co-delivery of antigens (from cell membrane) and adjuvant can enhance the immune response, with higher concentration of secreted cytokines IL-12p70 and IFN-γ (Fig. 2d and e). As reported, IL-12p70 activates $CD8^+$ T cells to generate IFN-γ to induce apoptosis in cancer cells [25]. According to the promising results in vitro, we further investigated the immunogenicity of CCMP@R837 in vivo.

Fig. 2. In vitro immunogenicity of CCMP@R837. a) Maturation ($CD86^+$ and $CD80^+$ positive BMDCs) of BMDCs treated with different formulations. b). Mechanism of in vitro antitumor effect of CCMP@R837. c) Effect of CCMP@R837 on 4T1 cell viability. d) and e) Effect of CCMP@R837 on IL-12p70 (d) and IFN-γ (e) secretion. Data represent mean ± SD (n =5; ***p < 0.001).

Immunogenicity of CCMP@R837 in vivo

For the in vivo experiments, we first investigated the biocompatibility of CCMP@R837 in healthy BALB/c mice. We vaccinated the BALB/c mice three times on day 0, 14 and 28 and recorded their body weight (Fig. S-2). Mice treated with different formulations exhibited similar trend in body weight (increasing body weight with time), indicating the long-term biocompatibility of CCMP@R837. After 31 days' immunization, 4T1 cells were subcutaneously injected into the right flank of these mice (Fig. 3a). We found that the tumor size in mice treated with saline, CCM and P@R837 dramatically increased after 14 days of injection, whereas for the mice treated using CCMP@R837, much less increase in tumor size was observed, indicating the significant suppress effect of CCMP@R837 in tumor progress (Fig. 3b-e). The average tumor size of the mice injected with saline, CCM and P@R837 were 6, 4.6, and 3 times higher than the CCMP@R837 immunized mice (Fig. 3f). Additionally, we can clearly see from the survival rate results: after 23 days of treatment, there were first death in saline, CCM and P@R837 groups, due to the aggressive tumor progress; The first death in the CCMP@R837 groups, however, happened 27 days after the 4T1 tumor cell injection. Additionally, the majority of mice in saline, CCM and P@R837 groups died between 20 days to 40 days after the

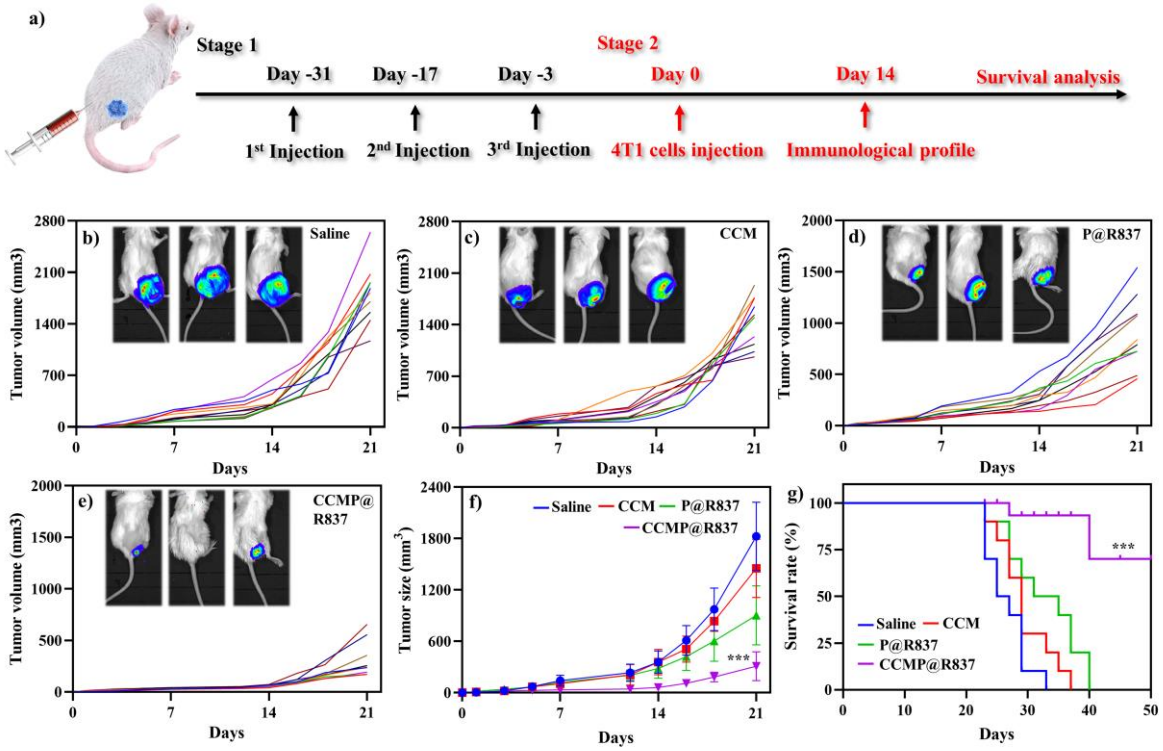

treatment. Moreover, for the CCMP@R837 group, 70% survival rate was observed after 50 days of treatment, with average tumor size of 379±103 mm^3. The above results have demonstrated the strong inhibition effect of tumor progress in the mice immunized with CCMP@R837.

Fig. 3 Antitumor effect of CCMP@R837 in vivo. a) Treatment plan for BALB/c mice. Individual tumor size in mice treated with b) saline, c) CCM, d) P@R837, and e) CCMP@R837. Every single line indicated individual BALB/c mice. f) Average tumor size of mice treated with various treatments. *** means the difference between CCMP@R836 groups and other groups at 21 days. g) Survival rate of BALB/c treated with different formulations. *** means the difference between CCMP@R836 groups and other groups at 50 days. Data represent mean ± SD (n =5; ***p < 0.001).

We further explored the underlying mechanism of the increasing survival rate and the inhibition of tumor growth in mice treated using CCMP@R837. Five mice were randomly selected from each group; spleen and tumor were collected for the immunological proliferation and investigation at 14 days post 4T1 cell injection. In this experiment, the serum was isolated from mice and the concentration of TNF-α in the

serum was investigated. TNF-α produced by $CD8^+$ CTLs is responsible for cancer cell elimination [26]. As shown in Fig. S-3, the TNF-α concentration in mice treated with CCMP@R837 was found 3, 1.5, and 4 times higher than that with CCM, P@R837 and silane. As known, CTLs play an important role in cleaning tumor cells by triggering the lysis of tumor cells. Thus, in the tumor tissue, the high percentage of CTLs indicates strong anti-tumor immune response for inhibition of tumor growth [27]. As shown in Fig. 4a, a significant population shift can be observed in the CTLs (positive expression of $CD3^+$ and $CD8^+$, $CD3^+$ is involved in activating both the cytotoxic T cells and T helper cells; $CD8^+$ is involved in the cytotoxic T cells) of CCMP@R837 groups. The percentage of CTLs in CCMP@R837 groups was found 1.9, 1.4, and 1.7 times higher than that in saline, P@R837 and CCM groups (Fig. 4b). In the tumor area, regulatory T cells (Tregs) are immunosuppressive and generally downregulate the proliferation of effector T cells [28]. Therefore, the Tregs ($CD4^+$, $Foxp3^+$) were investigated to evaluate the immunosuppression in BALB/c mice immunized with different formulations (Fig. 4c). Saline, CCM and P@R837 groups revealed 1.7, 1.5-, and 1.2-times higher percentage of Tregs in the tumor than the CCMP@R837 groups, respectively (Fig. 4d), which indicated that the BALB/c pre-immunized with CCMP@R837 have created less immune suppressive microenvironment than those treated with Saline, CCM and P@R837 groups [29]. We additionally examined the T cells' distribution in the tumor. As shown in Fig. 4e-g, plenty of $CD3^+$, $CD4^+$, and $CD8^+$ T cells were found in the tumor of BALB/c mice treated with CCMP@R837, revealing the strong cell-mediated immune responses.

The ability of CCMP@R837 in inducing the immune memory was further evaluated. After activation and antigen processing, $CD8^+$ T cells partially differentiate into memory T cells which can be further divided into central memory T cells (T_{CM}) and effector T cells (T_{EM}). In terms of functionality, T_{EM} can quickly play the role of fighting against tumor cells. As for the T_{CM}, it will be expanded when it is re-exposed to the cognate antigen [30]. In this study, spleen was collected to investigate the immunological profile in immunized BALB/c mice (Fig. 4h). We can see that the mice treated with CCMP@R837 showed a more significant shift of population from T_{CM} to T_{EM} compared to the mice treated with saline, CCM and P@R837, indicating activation of the anti-tumor effect. The higher number of T_{EM} in the spleen of CCMP@R837 immunized mice demonstrated that the majority of T cells were activated to fight against tumor cells (Fig. 4i). Overall, the increased survival rate and the inhibited tumor growth in mice treated with CCMP@R837 could mostly be contributed to the presence of higher percentage of $CD8^+$ T cells and lower percentage of Tregs in the tumor area. In addition, the presence of T_{EM} in the spleen of mice treated using CCMP@R837 also contributes to the inhibition of tumor growth. That is, our CCMP@R837 have enhanced the differentiation of $CD8^+$ T cells and T_{EM}, and inhibited the differentiation of Tregs, which ultimately facilitated the immunized mice fighting against tumor.

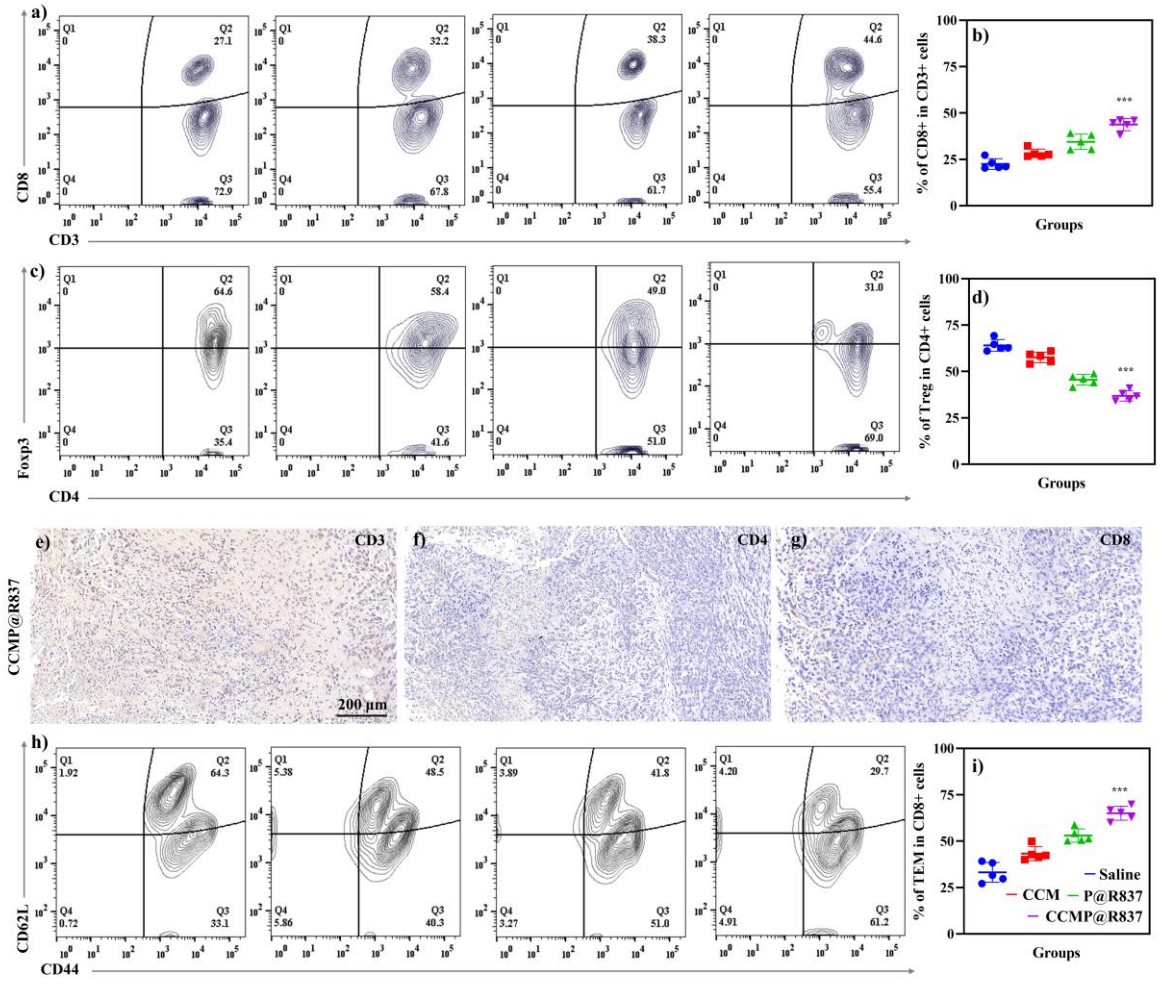

Fig. 4 Immunogenicity of CCMP@R837 in vivo. a) Flow cytometry results of tumor cell suspension in $CD3^+CD8^+$ T cells. b) Quantitative analysis of $CD3^+CD8^+$ T cells. c) Flow cytometry results of tumor cell suspension in $CD4^+Foxp3^+$ T cells. d) Quantitative analysis of $CD4^+Foxp3^+$ T cells. Presence of e) $CD3^+$ T cells, f) $CD4^+$ T cells, and g) $CD8^+$ T cells in tumor tissue in mice treated with CCMP@R837. h) Flow cytometry results of spleen cell suspension in $CD44^+CD62L^-$ T cells. i) Quantitative analysis of $CD44^+CD62L^-$ T cells. Data represent mean ± SD (n =5; ***p < 0.001).

Conclusions

In this work, we fabricated nanovaccines by combining PLGA, R837, and CCM. We demonstrated that our CCMP@R837 can effectively enhance the immunity and induce the generation of immune response to fight against breast cancer challenge. Compared with other pre-immunization treatments, such as saline, CCM and P@R837, our CCMP@R837 successfully trained the immune system of mice to be prepared for the 4T1 tumor challenge by boosting the maturation of antigen presenting cells, promoting the differentiation of CTLs and downregulating the precentage of Tregs in the tumor. The upregulated precentage of T_{EM} also plays a vital role in inhibiting tumor progress thanks to the full immune activation and resultant immune memory using our platform. Additionally, when the pre-immunized animals are challenged with 4T1 cancer cells, the T_{CM} and T_{EM} cells can quickly differentiate into CTLs to recognize and destroy cancer cells, with long-lasting anti-tumor immunity. For future study, it would be interesting to combine our platform with other therapy methods, such as photothermal therapy and irreversible electroporation to further enhance the therapeutic efficency.

Conflicts of interest

The authors declare no competing financial interest.

Author Contributions

L Xiao, Y Huang: Methodology; Y Yang: Writing - Original Draft; Z Miao: Validation; J Zhu, W Tang: Data curation; M Zhong, C Feng: Formal analysis; J Zhou: Resources; L Wang: Writing- Reviewing and Editing; X Zhao, Z Wang: Supervision

Acknowledgements

L. Xiao, Y. Huang, Y. Yang, Z. Miao contribute equally to this work. X. Zhao would like to acknowledge the General Research Fund (Grant no. 15202119) from Research Grants Council of Hong Kong and intra-faculty fund (1-ZVPC) from the Hong Kong Polytechnic University. Z.R. Wang would like to acknowledge the financial support from the National Nature Science Foundation of China (82074473) and the Natural Science Foundation of Jiangsu province (BK20191201).

References

1 J. Y. Zhu, D. W. Zheng, M. K. Zhang, W. Y. Yu, W. X. Qiu, J. J. Hu, J. Feng and X. Z. Zhang, Nano Lett., 2016, 16, 5895–5901.
2 Y. Min, K. C. Roche, S. Tian, M. J. Eblan, K. P. McKinnon, J. M. Caster, S. Chai, L. E. Herring, L. Zhang and T. Zhang, Nat. Nanotechnol., 2017, 12, 877–882.
3 A. V. Kroll, R. H. Fang, Y. Jiang, J. Zhou, X. Wei, C. L. Yu, J. Gao, B. T. Luk, D. Dehaini and W. Gao, Adv. Mater., 2017, 29, 1703969.
4 D. J. Schwartzentruber, D. H. Lawson, J. M. Richards, R. M. Conry, D. M. Miller, J. Treisman, F. Gailani, L. Riley, K. Conlon and B. Pockaj, N. Engl. J. Med., 2011, 364, 2119–2127.
5 Q. Chen, L. Xu, C. Liang, C. Wang, R. Peng and Z. Liu, Nat. Commun., 2016, 7, 1–13.
6 R. H. Fang, C. M. J. Hu, B. T. Luk, W. Gao, J. A. Copp, Y. Tai, D. E. O'Connor and L. Zhang, Nano Lett., 2014, 14, 2181–2188.
7 Y. Guo, D. Wang, Q. Song, T. Wu, X. Zhuang, Y. Bao, M. Kong, Y. Qi, S. Tan and Z. Zhang, ACS Nano, 2015, 9, 6918–6933.
8 R. Kuai, L. J. Ochyl, K. S. Bahjat, A. Schwendeman and J. J. Moon, Nat. Mater., 2017, 16, 489–496.
9 Y. Ye, C. Wang, X. Zhang, Q. Hu, Y. Zhang, Q. Liu, D. Wen, J. Milligan, A. Bellotti and L. Huang, Sci. Immunol., 2017, 2, eaan5692.
10 C. Wang, Y. Ye, Q. Hu, A. Bellotti and Z. Gu, Adv. Mater., 2017, 29, 1606036.
11 C. M. J. Hu, L. Zhang, S. Aryal, C. Cheung, R. H. Fang and L. Zhang, Proc. Natl. Acad. Sci. U. S. A., 2011, 108, 10980–10985.
12 C. M. J. Hu, R. H. Fang, B. T. Luk, K. N. Chen, C. Carpenter, W. Gao, K. Zhang and L. Zhang, Nanoscale, 2013, 5, 2664–2668.
13 J. Blonder, K. C. Chan, H. J. Issaq and T. D. Veenstra, Nat. Protoc., 2006, 1, 2784–2790.
14 W. L. Liu, M. Z. Zou, T. Liu, J. Y. Zeng, X. Li, W. Y. Yu, C. X. Li, J. J. Ye, W. Song and J. Feng, Nat. Commun., 2019, 10, 1–12.
15 H. Sun, J. Su, Q. Meng, Q. Yin, L. Chen, W. Gu, Z. Zhang, H. Yu, P. Zhang and S. Wang,Adv. Funct. Mater., 2017, 27, 1604300.
16 Y. Jiang, N. Krishnan, J. Zhou, S. Chekuri, X. Wei, A. V. Kroll, C. L. Yu, Y. Duan, W. Gao, R. H. Fang and L. Zhang, Advanced Materials, 2020, 32, 2001808.
17 R. Yang, J. Xu, L. Xu, X. Sun, Q. Chen, Y. Zhao, R. Peng and Z. Liu, Acs Nano, 2018,12, 5121–5129.
18 S. P. Kasturi, I. Skountzou, R. A. Albrecht, D. Koutsonanos, T. Hua, H. I. Nakaya, R. Ravindran, S. Stewart, M. Alam and M. Kwissa, Nature, 2011, 470, 543–547.

19 A. Madaan, R. Verma, A. T. Singh, S. K. Jain and M. Jaggi, Journal of Biological Methods, 2014, 1, e1.
20 S. Y. Li, H. Cheng, B. R. Xie, W. X. Qiu, J. Y. Zeng, C. X. Li, S. S. Wan, L. Zhang, W. L. Liu and X. Z. Zhang, ACS Nano, 2017, 11, 7006–7018.
21 J. A. Ledbetter, J. P. Deans, A. Aruffo, L. S. Grosmaire, S. B. Kanner, J. B. Bolen and G. L. Schieven, Curr. Opin. Immunol., 1993, 5, 334–340.
22 L. Miao, J. Li, Q. Liu, R. Feng, M. Das, C. M. Lin, T. J. Goodwin, O. Dorosheva, R. Liu and L. Huang, ACS Nano, 2017, 11, 8690–8706.
23 F. Fontana, M. Fusciello, C. Groeneveldt, C. Capasso, J. Chiaro, S. Feola, Z. Liu, E. M. Mäkilä, J. J. Salonen and J. T. Hirvonen, ACS Nano, 2019, 13, 6477–6490.
24 A. S. Cheung, S. T. Koshy, A. G. Stafford, M. M. Bastings and D. J. Mooney, Small, 2016, 12, 2321–2333.
25 L. Escribà-Garcia, C. Alvarez-Fernández, M. Tellez-Gabriel, J. Sierra and J. Briones, J. Transl. Med., 2017, 15, 115.
26 A. Ratner and W. R. Clark, J. Immunol., 1993, 150, 4303–4314.
27 Y. Cao, Y. H. Feng, L. W. Gao, X. Y. Li, Q. X. Jin, Y. Y. Wang, Y. Y. Xu, F. Jin, S. L. Lu and M. J. Wei, Int. Immunopharmacol., 2019, 70, 110–116.
28 T. J. Curiel, The Journal of Clinical Investigation, 2007, 117, 1167–1174.
29 D. H. Munn and V. Bronte, Curr. Opin. Immunol., 2016, 39, 1–6.
30 M. Pepper and M. K. Jenkins, Nat. Immunol., 2011, 12, 467–471.